Rapid Communications

# Nonlocal emergent hydrodynamics in a long-range quantum spin system

Alexander Schuckert,* Izabella Lovas,† and Michael Knap‡
*Department of Physics and Institute for Advanced Study, Technical University of Munich, D-85748 Garching, Germany and Munich Center for Quantum Science and Technology (MCQST), Schellingstrasse 4, D-80799 München, Germany*

(Received 7 September 2019; published 28 January 2020)

Generic short-range interacting quantum systems with a conserved quantity exhibit universal diffusive transport at late times. We employ nonequilibrium quantum field theory and semiclassical phase-space simulations to show how this universality is replaced by a more general transport process in a long-range XY spin chain at infinite temperature with couplings decaying algebraically with distance as $r^{-\alpha}$. While diffusion is recovered for $\alpha > 1.5$, longer-ranged couplings with $0.5 < \alpha \leqslant 1.5$ give rise to effective classical Lévy flights, a random walk with step sizes drawn from a distribution with algebraic tails. We find that the space-time-dependent spin density profiles are self-similar, with scaling functions given by the stable symmetric distributions. As a consequence, for $0.5 < \alpha \leqslant 1.5$, autocorrelations show hydrodynamic tails decaying in time as $t^{-1/(2\alpha-1)}$ and linear-response theory breaks down. Our findings can be readily verified with current trapped ion experiments.

DOI: 10.1103/PhysRevB.101.020416

In quantum many-body systems, macroscopic inhomogeneities in a conserved quantity must be transported across the whole system to reach an equilibrium state. As this is in general a slow process compared to local dephasing, essentially *classical* hydrodynamics is expected to emerge at late times in the absence of long-lived quasiparticle excitations [1–8]. The universality of this effective classical description may be understood from the central limit theorem: In the regime of incoherent transport, short-range interactions lead to an effective random walk with a finite variance of step sizes, leading to a Gaussian distribution at late times. This universality is only broken when quantum coherence is retained, such as in integrable models [9–15] or in the vicinity of a many-body localized phase, where rare region effects give rise to subdiffusive transport [16–22].

In this Rapid Communication, we show how this universal diffusive transport in short-range interacting systems is replaced by a more general, nonlocal effective hydrodynamical description in systems with algebraically decaying long-range interactions. We use semianalytical nonequilibrium quantum field theory calculations (referred to as spin-2PI below) and a discrete truncated Wigner approximation (dTWA) to show that in a long-range interacting XY spin chain, spin transport at infinite temperature effectively obeys a classical master equation with *long-range*, algebraically decaying transition amplitudes. This effective description can be reformulated as a classical random walk with an infinite variance of step sizes, giving rise to a generalized central limit theorem and to a late-time description in terms of classical Lévy flights [23], an example for *superdiffusive* anomalous transport. As a result, we demonstrate that the full spatiotemporal shape of the correlation function $C(j,t) = \langle \hat{S}^z_j(t)\hat{S}^z_0(0)\rangle$, and, in particular, the exponent of the hydrodynamic tail in the autocorrelation function $C(j=0,t)$, depends strongly on the long-range exponent $\alpha$. While for $\alpha > 1.5$ we recover classical diffusion, the autocorrelation function shows hydrodynamic tails with an exponent $1/(2\alpha - 1)$ for $0.5 < \alpha \leqslant 1.5$, as we show in Fig. 1. Furthermore, $C(j,t)$ possesses a self-similar behavior,

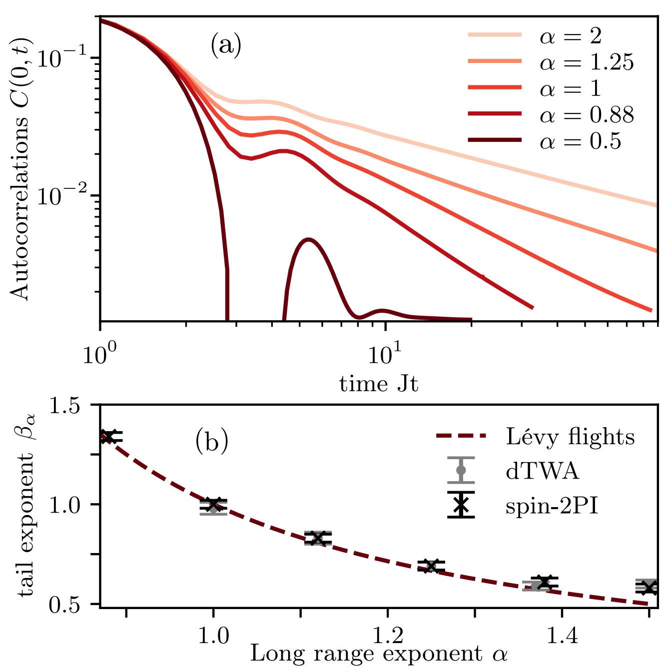


FIG. 1. Hydrodynamic tails in the spin autocorrelator. (a) For long-range coupling exponents $\alpha > 0.5$, autocorrelations decay algebraically at late times with an exponent that depends on $\alpha$. By contrast, for $\alpha \leqslant 0.5$, hydrodynamic tails are absent. (b) The exponents $\beta_\alpha$ of the hydrodynamic tail obtained from two different approaches (symbols) agree with the predictions from classical Lévy flights in the thermodynamic limit (dashed curve). Deviations at large $\alpha$ are due to finite-time corrections to scaling which can also be understood from Lévy flights.

*alexander.schuckert@tum.de
†izabella.lovas@tum.de
‡michael.knap@ph.tum.de

 

with the scaling function covering all stable symmetric distributions as a function of $\alpha$, smoothly crossing over from a Gaussian at $\alpha = 1.5$ over a Lorentzian at $\alpha = 1$ to an even more sharply peaked function as $\alpha \to 0.5$. We also extract the generalized diffusion coefficient $D_\alpha$ from the scaling functions, and explain its $\alpha$ dependence by Lévy flights; quantum effects are incorporated in a many-body timescale depending only weakly on $\alpha$. For $\alpha \leqslant 0.5$ no emergent hydrodynamic behavior is found as the system relaxes instantaneously in the thermodynamic limit [24].

This Rapid Communication not only shows how nonlocal transport phenomena emerge in long-range interacting systems, but also establishes both nonequilibrium quantum field theory and discrete truncated Wigner simulations as efficient tools to study transport phenomena in the thermalization dynamics of quantum many-body systems.

*Model.* We study the long-range interacting quantum XY chain with open boundary conditions, given by the Hamiltonian

$$\hat{H} = -\frac{1}{2} \sum_{i \neq j = -L/2}^{L/2} \frac{J}{\mathcal{N}_{L,\alpha} |i-j|^\alpha} \left( \hat{S}_i^x \hat{S}_j^x + \hat{S}_i^y \hat{S}_j^y \right). \quad (1)$$

Here, $\hat{S}^\alpha = \frac{1}{2}\hat{\sigma}^\alpha$ denotes spin-$\frac{1}{2}$ operators given in terms of Pauli matrices, $L$ is the (odd) length of the chain [25], and we set $\hbar = 1$. The interaction strength $J$ is rescaled with the factor $\mathcal{N}_{L,\alpha} = \sqrt{\sum_{j \neq 0} |j|^{-2\alpha}}$ in order to remove the $L$ and $\alpha$ dependence of the timescale associated with the perturbative short-time dynamics of the central spin at $i = 0$. The above model shows chaotic (Wigner-Dyson) level statistics for the whole range of $\alpha$ considered here ($0.5 \leqslant \alpha \leqslant 2$) and is an effective description of the long-range transverse field Ising model for large fields [26,27]. In particular, it conserves the total $S^z$ magnetization, with product states in the $S^z$ basis evolving radically differently depending on the complexity of the corresponding magnetization sector. For just a few spin flips on top of the completely polarized state, the dynamics can be exactly solved and are described in terms of ballistically propagating spin waves, with a diverging group velocity at $\alpha = 1$ [26,28,29] related to the algebraic leakage of the Lieb-Robinson bound [30–33]. In contrast, here we show that the exponentially large Hilbert space sector for an extensive number of spin flips gives rise to rich transport phenomena, driven by the long-range nature of the interactions.

*Effective stochastic description of long-range transport.* As the model in Eq. (1) is equivalent to long-range hopping hard core bosons, we conjecture the effective classical equation of motion for the transported local density $f_j(t)$, in our case $\langle \hat{S}_j^z(t) \rangle + \frac{1}{2}$, to be of the form [34]

$$\partial_t f_j(t) = \sum_{i \neq j} [W_{i \to j} f_i (1 - f_j) - W_{j \to i} f_j (1 - f_i)]. \quad (2)$$

Here, the transition rate $W_{i \to j}$ is determined by the microscopic transport processes present in the Hamiltonian, in our case the long-range hopping of spins. More specifically, from Fermi's golden rule, the transition rate for a flip-flop process between spins $i$ and $j$ is proportional to $|\langle \uparrow_i \downarrow_j | \hat{H} | \downarrow_i \uparrow_j \rangle|^2$, and hence we phenomenologically set

$$W_{i \to j} = W_{j \to i} = \frac{\lambda}{|i-j|^{2\alpha}}, \quad (3)$$

where $\lambda^{-1}$ is a characteristic timescale determined by the full many-body Hamiltonian.

Starting from an initial state with a single excitation in the center of the chain, the solution of this master equation is given by [35]

$$f_j(t) \approx \begin{cases} (D_\alpha t)^{-1/2}\, G\left(\frac{|j|}{(D_\alpha t)^{1/2}}\right) & \text{for } \alpha > 1.5, \\ (D_\alpha t)^{-\beta_\alpha} F_\alpha\left(\frac{|j|}{(D_\alpha t)^{\beta_\alpha}}\right) & \text{for } 0.5 < \alpha \leqslant 1.5, \end{cases} \quad (4)$$

in the limit of long times and large system sizes. Here, $G(y) = \exp(-y^2/4)/8\sqrt{\pi}$ denotes the Gaussian distribution, indicating normal diffusion for $\alpha > 1.5$ with a diffusion constant $D_\alpha \propto \lambda$. For $0.5 < \alpha \leqslant 1.5$, $G(y)$ is replaced by the family of stable, symmetric distributions $F_\alpha(y)$, given by

$$F_\alpha(y) = \frac{1}{4} \int \frac{dk}{2\pi} \exp(-|k|^{1/\beta_\alpha}) \exp(iyk), \quad (5)$$

with the constant prefactor $D_\alpha = \lambda c_\alpha$ constituting a generalized diffusion coefficient [36]. We find $c_\alpha = -2\Gamma(1 - 2\alpha)\sin(\pi\alpha)$ from the classical master equation, with $\Gamma$ denoting the gamma function [35]. Furthermore, the exponent of the hydrodynamic tail $\beta_\alpha$ is given by

$$\beta_\alpha = \frac{1}{2\alpha - 1}. \quad (6)$$

The Fourier transform in Eq. (5) only leads to elementary functions for $\alpha = 3/2$ and $\alpha = 1$, resulting in a Gaussian and a Lorentzian distribution, respectively [37]. The scaling functions $F_\alpha(y)$ are the fixed point distributions in the generalized central limit theorem [38] of independent and identically distributed (i.i.d.) random variables with heavy tailed distributions. Importantly, $F_\alpha(y)$ has diverging variance for $\alpha < 1.5$, undefined mean for $\alpha \leqslant 1$, and displays heavy tails $\sim |y|^{-2\alpha}$. The classical master equation hence predicts a crossover from diffusive ($\alpha \geqslant 1.5$) over ballistic ($\alpha = 1$) to superballistic ($0.5 < \alpha < 1$) transport.

When adding a linear magnetic field gradient $\sim E \sum_i i\hat{S}_i^z$ to the Hamiltonian, the resulting classical master equation predicts the spin current to depend nonlinearly on the arbitrarily weak $E$ for $\alpha < 1.5$, indicating a breakdown of linear-response theory [35,39]. Calculating the current response function from Eq. (4), we find a diverging response for vanishing momentum $q \to 0$ for every value of the frequency $\omega$ [35,40].

*Quantum dynamics from spin-2PI and dTWA.* In the following, we demonstrate the emergence of these effective classical dynamics in the quantum dynamics of the Hamiltonian (1), by studying the unequal-time correlation function

$$C(j,t) := \mathrm{Tr}\left[\hat{S}_j^z(t)\hat{S}_0^z(0)\right]_{|j=0\rangle = |\uparrow\rangle}. \quad (7)$$

Here, we perform the trace over product states in the $S^z$ basis, restricted to the Hilbert space sector with $\sum_i S_i^z = \frac{1}{2}$, such that $\langle S_i^z(t=0) \rangle = \frac{1}{2}\delta_{0,i}$ for all spins $i$. This way, we probe the transport of a single spin excitation moving in an infinite-temperature bath with vanishing total magnetization.

We employ two complementary, approximate methods to study the dynamics at long times and for large system sizes, in a regime that is challenging to access by numerically exact methods [41]. Schwinger boson spin-2PI [42,43], a nonequilibrium quantum field theory method, employs an expansion in the inverse coordination number $1/z$ to reduce the many-body problem to solving an integrodifferential equation that scales algebraically in system size. As the effective coordination number is large in a long-range interacting system, we expect this approximation to be valid for small $\alpha$. The discrete truncated Wigner approximation evolves the classical equations of motion, while introducing quantum fluctuations by sampling initial states from the Wigner distribution [44–47] and was shown to be particularly well suited for studying long-range interacting systems [46,48]. In both methods, we evaluate $C(j,t)$ by starting from random initial product states in the $S^z$ basis and then averaging over sufficiently many such initial states [49]. If not stated otherwise, all our results have been converged with respect to system size, for which we employed chains with 201–601 sites.

We study two distinct regimes in the dynamics. A perturbative short-time regime characterized by initial dephasing is followed by the emergent effective classical long-range transport described by the master equation.

*Perturbative short-time dynamics.* At short times, second-order perturbation theory yields

$$\mathrm{Tr}\left[\hat{S}^z_j(t)\hat{S}^z_0(0)\right] \approx \begin{cases} \frac{1}{4}\left(1-\frac{J^2t^2}{4}\right) & \text{for } j=0, \\ \left(\frac{Jt}{4\mathcal{N}_{L,\alpha}}\right)^2\frac{1}{|j|^{2\alpha}} & \text{for } j\neq 0. \end{cases} \tag{8}$$

Physically, in this regime each spin is precessing in the effective magnetic field created by all other spins. The autocorrelation function is independent of $\alpha$ and $L$ due to our choice of the normalization factor $\mathcal{N}_{L,\alpha}$, ensuring that the typical magnetic field at the center of the chain remains of the order of $J$. The spatial correlation function at a fixed time inherits the algebraic behavior of the interaction strength, falling off as $|j|^{-2\alpha}$ between spins of distance $j$, which is reproduced by both dTWA (not shown) and spin-2PI (see Fig. 2).

*Hydrodynamic tails.* The scaling form from classical Lévy flights in Eq. (4) implies the presence of a hydrodynamic tail in the autocorrelation function $C(j=0,t)$ with exponent $\beta_\alpha = 1/(2\alpha-1)$, which replaces the universal exponent 1/2 for diffusion in one dimension (1D) (see Fig. 1 for our field theory results). For $\alpha \to 1.5$ we find slight deviations from $\beta_\alpha$, but these can, however, be explained by a subtle finite-time effect also present in classical Lévy flights [35]. For $\alpha < 0.5$ we find no hydrodynamic tail for the numerically accessible system sizes $L < 601$. This matches the expectation that the system relaxes instantaneously in the thermodynamic limit [24], which is also indicated by the fact that the perturbative short timescale diverges, $\mathcal{N}_{L\to\infty,\alpha} = \infty$, for $\alpha \leqslant 0.5$. On even longer timescales, the discretized Fourier transform underlying the derivation of Eq. (4) is dominated by the smallest wave number in finite chains, and the hydrodynamic tail is replaced by an exponential convergence towards the equilibrium value $0.25/L$ with a rate $\sim(1/L)^{2\alpha-1}$.

*Self-similar time evolution of correlations.* In Fig. 3 we show the spreading of $t^{\beta_\alpha}C(j,t)$ for two values of $\alpha$. While for $\alpha = 2$ a diffusive cone is visible, the spreading for $\alpha = 1$

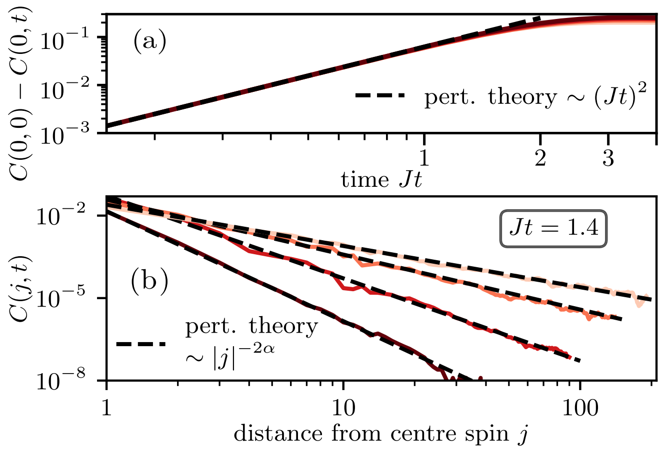


FIG. 2. Short-time dynamics. We compare spin-2PI results with second-order perturbation theory, Eq. (8). (a) The collapse of the autocorrelator for different exponents $\alpha$ shows that the short-time evolution is independent of $\alpha$ and $L$ when the Hamiltonian is rescaled with $\mathcal{N}_{\alpha,L}$. (b) The unequal-time correlation function for $\alpha \in \{0.75, 1, 1.5, 2\}$ (from top to bottom), shows algebraic tails that are entirely captured by second-order perturbation theory. We used a moving average over five to ten lattice sites to smoothen the results.

is ballistic, as expected from the master equation. The scaling collapse of these data shows good agreement with classical Lévy flights [Eq. (4)] at late times. Interestingly, we find heavy tails even for $\alpha \geqslant 1.5$. We explain these by subleading corrections to the scaling ansatz Eq. (4) present in the master equation [35]. They survive up to algebraically long times for $\alpha > 1.5$, turning to a logarithmic correction at $\alpha = 1.5$ [50].

For $\alpha \gtrsim 2$ we furthermore find signs of peaks propagating ballistically for intermediate times in the dTWA scaling functions, which survive longer as $\alpha$ increases. These peaks are remnants of the integrable point at $\alpha = \infty$ [35]. Such behavior is not present in the spin-2PI data as this method is not able to capture integrable behavior [43].

*Generalized diffusion constant.* The only free parameter of our effective classical description is the generalized diffusion coefficient $D_\alpha$, which we obtain from the fits to the scaling function. In Fig. 4 we show that the leading $\alpha$ dependence of $D_\alpha$ can be explained by $D_\alpha \sim c_\alpha$ for $\alpha < 1.5$ [51], hence the prefactor $\lambda^{-1}$, constituting the *quantum* many-body time scale, depends only weakly on $\alpha$. As expected from their differing approximate treatment of the quantum fluctuations in the system, we find slight differences between the values of $\lambda$ determined by spin-2PI and dTWA, $\lambda_{\mathrm{2PI}} \approx 0.25$ and $\lambda_{\mathrm{dTWA}} \approx 0.15$. For $\alpha > 1.5$ we find considerable differences between the dTWA and spin-2PI results, because the emergent ballistic peaks, stemming from the nearby integrable point, accelerate the spreading in the dTWA simulations.

*Conclusions.* In this Rapid Communication, we have shown that spin transport at high temperatures in long-range interacting XY chains is well described by Lévy flights for long-range interaction exponents $0.5 < \alpha \leqslant 1.5$, effectively realizing a random walk with an infinite variance of step sizes. In particular, we have shown that the scaling function of the unequal time spin correlation function covers the stable symmetric distributions, in accordance with the

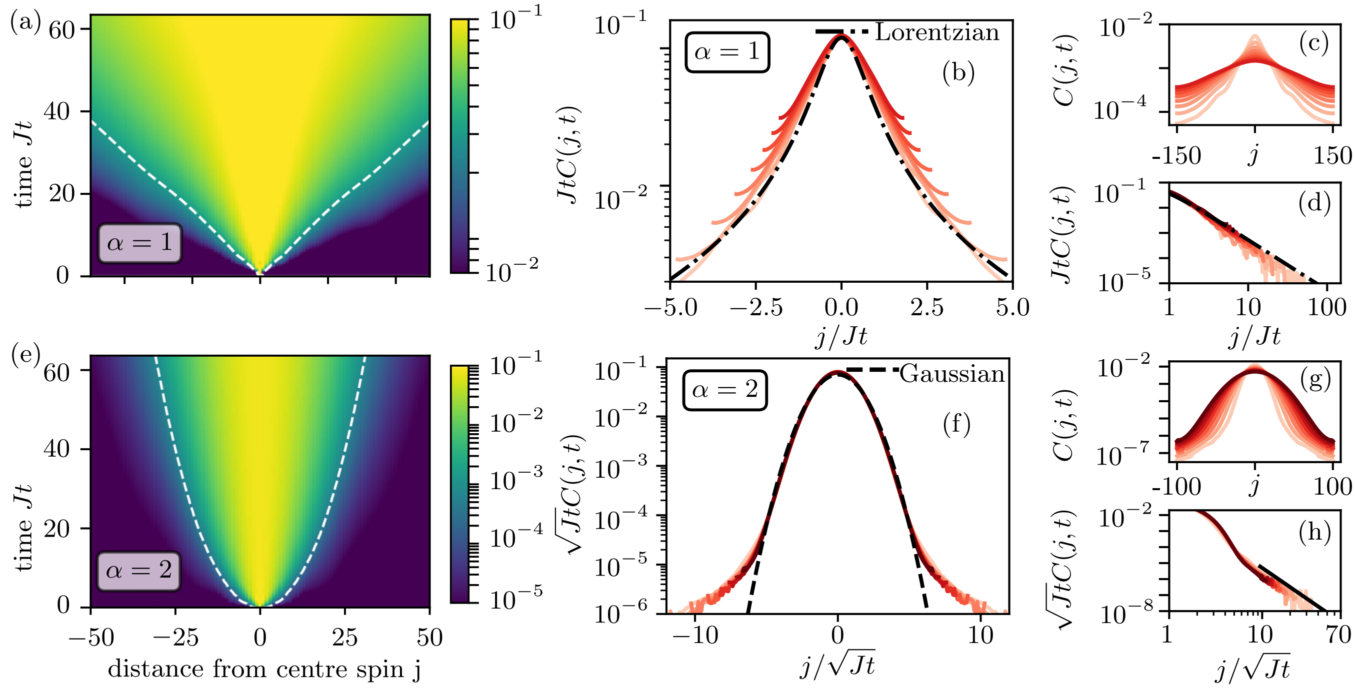


FIG. 3. Emergent self-similar time evolution. The correlation function $C(j,t)$ obtained from spin-2PI for chains of lengths $L = 201$ [(e)–(h) $\alpha = 2$], $L = 301$ [(a)–(d) $\alpha = 1$]. (a), (e) $C(j,t)$ multiplied by $t^{1/(2\alpha-1)}$ to account for the overall decay expected from Lévy flights shows a diffusive cone for $\alpha = 2$, whereas for $\alpha = 1$ a ballistic light cone emerges. The contour lines for $\alpha = 1, 2$ correspond to values $t^{1/(2\alpha-1)}C(j,t) = 0.03,\ 10^{-4}$, respectively. (b), (f) Rescaling of linearly spaced time slices for $23 \leqslant Jt \leqslant 84$ ($\alpha = 1$) and $42 \leqslant Jt \leqslant 226$ ($\alpha = 2$) (lines become darker as time increases) for the same data as in (a) and (e) agrees well with the scaling function expected from classical Lévy flights [Eq. (4)]. The only fitting parameter is the generalized diffusion coefficient. (d), (h) Rescaled time slices ($2 \leqslant Jt \leqslant 28$) on a double-logarithmic scale reveal for $\alpha = 1$ the heavy tail $\sim y^{-2}$ expected from Lévy flights [Eq. (4)], where the dashed-dotted line is the same fit as in (b). The tail $\sim y^{-4}$ (thick black line) for $\alpha = 2$ ($8 \leqslant Jt \leqslant 85$) is a finite-time effect also present in classical Lévy flights. (c), (g) Unscaled data.

generalized central limit theorem. While the system relaxes instantly for $\alpha < 0.5$, standard diffusion was recovered for $\alpha > 1.5$, with heavy tails from finite-time corrections surviving until extremely long times. We demonstrated the nontrivial dependence of the generalized diffusion coefficient $D_\alpha$ on $\alpha$, and found that it is captured by classical Lévy flights, with the quantum many-body timescale being approximately independent of $\alpha$. While we only studied one-dimensional systems, we expect this phenomenon to generalize straightforwardly to $d > 1$ dimensions. Assuming the effective classical Lévy flight picture persists, superdiffusive behavior would be found for $d/2 < \alpha < 1 + d/2$ with the exponent of the hydrodynamic tails given by $d/(2\alpha - d)$ [35]. Furthermore, we indicated that Lévy flights also imply a nonlinear response of the spin current to magnetic field gradients.

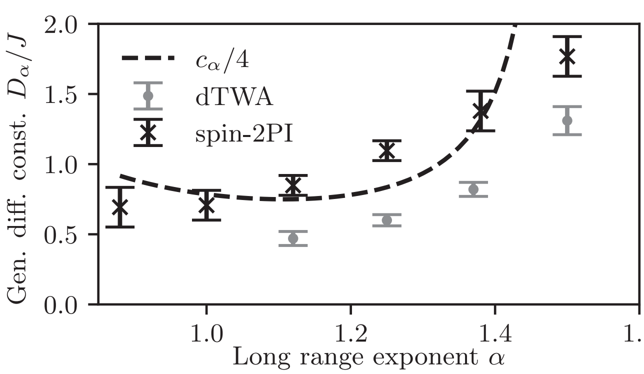


FIG. 4. Generalized diffusion constant. The $\alpha$ dependence of the diffusion constant obtained from fits with the scaling function of Lévy flights [Eq. (4)]. The qualitative behavior follows the Lévy flight prediction $D_\alpha \sim c_\alpha$ for $\alpha < 1.5$.

The long-range transport process found here can be experimentally studied in current trapped ion experiments [52], which can reach the required timescales [53–56]. The effective infinite-temperature states can also be realized by sampling over random product states which are then evolved in time.

*Acknowledgments.* We thank Rainer Blatt, Eleanor Crane, Iliya Esin, Philipp Hauke, Christine Maier, Asier Piñeiro Orioli, Tibor Rakovszky, and Achim Rosch for insightful discussions and the Nanosystems Initiative Munich (NIM) funded by the German Excellence Initiative for access to their computational resources. We acknowledge support from the Max Planck Gesellschaft (MPG) through the International Max Planck Research School for Quantum Science and Technology (IMPRS-QST), the Technical University of Munich - Institute for Advanced Study, funded by the German Excellence Initiative and the European Union FP7 under Grant Agreement No. 291763, the Deutsche Forschungsgemeinschaft (DFG, German Research Foundation) under Germany's Excellence Strategy–EXC-2111–390814868, and the European Research Council (ERC) under the European Union's Horizon 2020 research and innovation programme (Grant Agreements No. 771537 and No. 851161), from DFG Grant No. KN1254/1-1, and DFG TRR80 (Project F8).


[1] S. Mukerjee, V. Oganesyan, and D. Huse, Phys. Rev. B **73**, 035113 (2006).
[2] J. Lux, J. Müller, A. Mitra, and A. Rosch, Phys. Rev. A **89**, 053608 (2014).
[3] A. Bohrdt, C. B. Mendl, M. Endres, and M. Knap, New J. Phys. **19**, 063001 (2017).
[4] M. Medenjak, K. Klobas, and T. Prosen, Phys. Rev. Lett. **119**, 110603 (2017).
[5] E. Leviatan, F. Pollmann, J. H. Bardarson, D. A. Huse, and E. Altman, arXiv:1702.08894.
[6] V. Khemani, A. Vishwanath, and D. A. Huse, Phys. Rev. X **8**, 031057 (2018).
[7] T. Rakovszky, F. Pollmann, and C. W. von Keyserlingk, Phys. Rev. X **8**, 031058 (2018).
[8] D. E. Parker, X. Cao, A. Avdoshkin, T. Scaffidi, and E. Altman, Phys. Rev. X **9**, 041017 (2019).
[9] O. A. Castro-Alvaredo, B. Doyon, and T. Yoshimura, Phys. Rev. X **6**, 041065 (2016).
[10] B. Bertini, M. Collura, J. De Nardis, and M. Fagotti, Phys. Rev. Lett. **117**, 207201 (2016).
[11] S. Gopalakrishnan and R. Vasseur, Phys. Rev. Lett. **122**, 127202 (2019).
[12] M. Ljubotina, L. Zadnik, and T. Prosen, Phys. Rev. Lett. **122**, 150605 (2019).
[13] M. Ljubotina, M. Žnidarič, and T. Prosen, Phys. Rev. Lett. **122**, 210602 (2019).
[14] P. Prelovšek, J. Bonča, and M. Mierzejewski, Phys. Rev. B **98**, 125119 (2018).
[15] M. Środa, P. Prelovšek, and M. Mierzejewski, Phys. Rev. B **99**, 121110(R) (2019).
[16] K. Agarwal, S. Gopalakrishnan, M. Knap, M. Müller, and E. Demler, Phys. Rev. Lett. **114**, 160401 (2015).
[17] Y. Bar Lev, G. Cohen, and D. R. Reichman, Phys. Rev. Lett. **114**, 100601 (2015).
[18] R. Vosk, D. A. Huse, and E. Altman, Phys. Rev. X **5**, 031032 (2015).
[19] A. C. Potter, R. Vasseur, and S. A. Parameswaran, Phys. Rev. X **5**, 031033 (2015).
[20] P. Bordia, H. Lüschen, S. Scherg, S. Gopalakrishnan, M. Knap, U. Schneider, and I. Bloch, Phys. Rev. X **7**, 041047 (2017).
[21] S. Gopalakrishnan, K. R. Islam, and M. Knap, Phys. Rev. Lett. **119**, 046601 (2017).
[22] K. Agarwal, E. Altman, E. Demler, S. Gopalakrishnan, D. A. Huse, and M. Knap, Ann. Phys. **529**, 1600326 (2017).
[23] V. Zaburdaev, S. Denisov, and J. Klafter, Rev. Mod. Phys. **87**, 483 (2015).
[24] R. Bachelard and M. Kastner, Phys. Rev. Lett. **110**, 170603 (2013).
[25] We always assume integer divisions when we write $\frac{L}{2}$.
[26] P. Jurcevic, B. P. Lanyon, P. Hauke, C. Hempel, P. Zoller, R. Blatt, and C. F. Roos, Nature (London) **511**, 202 (2014).
[27] J. Smith, A. Lee, P. Richerme, B. Neyenhuis, P. W. Hess, P. Hauke, M. Heyl, D. A. Huse, and C. Monroe, Nat. Phy. **12**, 907 (2016).
[28] P. Hauke and L. Tagliacozzo, Phys. Rev. Lett. **111**, 207202 (2013).
[29] P. Richerme, Z.-X. Gong, A. Lee, C. Senko, J. Smith, M. Foss-Feig, S. Michalakis, A. V. Gorshkov, and C. Monroe, Nature (London) **511**, 198 (2014).
[30] E. H. Lieb and D. W. Robinson, Commun. Math. Phys. **28**, 251 (1972).
[31] M. B. Hastings and T. Koma, Commun. Math. Phys. **265**, 781 (2006).
[32] J. Eisert, M. van den Worm, S. R. Manmana, and M. Kastner, Phys. Rev. Lett. **111**, 260401 (2013).
[33] M. C. Tran, A. Y. Guo, Y. Su, J. R. Garrison, Z. Eldredge, M. Foss-Feig, A. M. Childs, and A. V. Gorshkov, Phys. Rev. X **9**, 031006 (2019).
[34] A master equation in terms of a local *probability* density may be obtained by normalizing the local density.
[35] See Supplemental Material at http://link.aps.org/supplemental/10.1103/PhysRevB.101.020416 for a derivation and discussion of the scaling functions from the classical master equation in dimension $d = 1, 2, 3$, a discussion of finite size effects in the autocorrelation function and corrections to scaling for finite times, a discussion of the integrable limit $\alpha \to \infty$ as well as a derivation of the connection of the spin conductivity to the correlation function and the breakdown of linear response within the classical master equation.
[36] The prefactor 1/4 accounts for the normalization of the correlation function, $C(j, t = 0) = \delta_{0,j}/4$. Furthermore, reinstating a lattice spacing $a$, the units of $D_\alpha$ depend on $\alpha$, in particular, it is a velocity for $\alpha = 1$.
[37] Other closed form solutions exist [57], for example, for $\alpha = 1.25$ in terms of hypergeometric functions.
[38] B. Gnedenko and A. N. Kolmogorov, *Limit Distributions for Sums of Independent Random Variables* (Addison-Wesley, Boston, 1954).
[39] V. E. Arkhincheev, in *Disordered and Complex Systems*, edited by A. C. C. Coolen, P. Sollich, R. F. Streater, and L. P. Hughston, AIP Conf. Proc. No. 553 (AIP, New York, 2001), p. 231.
[40] D. Forster, *Hydrodynamic Fluctuations, Broken Symmetry, And Correlation Functions* (Westview Press, Boulder, CO, 1994).
[41] B. Kloss and Y. Bar Lev, Phys. Rev. A **99**, 032114 (2019).
[42] M. Babadi, E. Demler, and M. Knap, Phys. Rev. X **5**, 041005 (2015).
[43] A. Schuckert, A. Piñeiro Orioli, and J. Berges, Phys. Rev. B **98**, 224304 (2018).
[44] W. K. Wootters, Ann. Phys. **176**, 1 (1987).
[45] A. Polkovnikov, Ann. Phys. **325**, 1790 (2010).
[46] J. Schachenmayer, A. Pikovski, and A. M. Rey, Phys. Rev. X **5**, 011022 (2015).
[47] L. Pucci, A. Roy, and M. Kastner, Phys. Rev. B **93**, 174302 (2016).
[48] A. P. Orioli, A. Signoles, H. Wildhagen, G. Günter, J. Berges, S. Whitlock, and M. Weidemüller, Phys. Rev. Lett. **120**, 063601 (2018).

[49] In spin-2PI simulations we used 4–16 different initial states, while in dTWA the averaging over initial states is performed in parallel with the Monte Carlo averaging over the Wigner distribution; here, we typically use $\sim 10^5$ samples.

[50] L. Zarfaty, A. Peletskyi, E. Barkai, and S. Denisov, Phys. Rev. E **100**, 042140 (2019).

[51] The spurious divergence of $c_\alpha$ in the limit $\alpha = 1.5$ is cured by logarithmic corrections to scaling [35]. Furthermore, without the normalization $N_{L,\alpha}$, $D(\alpha) \sim N_{L,\alpha} \to \infty$ for $\alpha \to 0.5$.

[52] D. Porras and J. I. Cirac, Phys. Rev. Lett. **92**, 207901 (2004).

[53] T. Brydges, A. Elben, P. Jurcevic, B. Vermersch, C. Maier, B. P. Lanyon, P. Zoller, R. Blatt, and C. F. Roos, Science **364**, 260 (2019).

[54] J. Zhang, G. Pagano, P. W. Hess, A. Kyprianidis, P. Becker, H. Kaplan, A. V. Gorshkov, Z.-X. Gong, and C. Monroe, Nature (London) **551**, 601 (2017).

[55] N. Friis, O. Marty, C. Maier, C. Hempel, M. Holzäpfel, P. Jurcevic, M. B. Plenio, M. Huber, C. Roos, R. Blatt, and B. Lanyon, Phys. Rev. X **8**, 021012 (2018).

[56] C. Maier, T. Brydges, P. Jurcevic, N. Trautmann, C. Hempel, B. P. Lanyon, P. Hauke, R. Blatt, and C. F. Roos, Phys. Rev. Lett. **122**, 050501 (2019).

[57] W. H. Lee, Continuous and discrete properties of stochastic processes, Ph.D. thesis, University of Nottingham, 2010.